Quaternary Science Reviews 28 (2009) 80–92

Contents lists available at ScienceDirect

Quaternary Science Reviews

journal homepage: www.elsevier.com/locate/quascirev

Stromatolites in caves of the Dead Sea Fault Escarpment: implications to latest Pleistocene lake levels and tectonic subsidence

Sorin Lisker [a,*], Anton Vaks [b,c], Miryam Bar-Matthews [b], Roi Porat [a], Amos Frumkin [a]

[a] Cave Research Unit, Department of Geography, The Hebrew University of Jerusalem, Mount Scopus Campus, Jerusalem 91905, Israel
[b] Geological Survey of Israel, 30 Malchkei Yisrael St., Jerusalem 95501, Israel
[c] Department of Earth Sciences, University of Oxford, Park Road, Oxford, UK

ARTICLE INFO

Article history:
Received 20 December 2007
Received in revised form
23 September 2008
Accepted 6 October 2008

ABSTRACT

A varied assemblage of algal stromatolites was encountered in caves along the northern section of the Dead Sea Fault Escarpment. The caves are situated at the lower part of the escarpment at altitudes −310 to −188 m relative to mean sea level (m.s.l.), i.e. ca 110–230 m above the present Dead Sea level. The cave stromatolites are mainly composed of aragonite yielding U–Th ages of ~75–17 ka. The altitude, mineralogy and ages, as well as comparison with previously documented stromatolite outcrops in the area, ascribe the cave stromatolites to the aragonite-precipitating hypersaline Lake Lisan—the Late Pleistocene predecessor of the Dead Sea.

The stromatolites are used as a lake level gauge, based on the algae being reliant upon the light of the upper water layer. Preservation of the original structure and aragonite mineralogy of the stromatolites, suggests a closed system regarding the radioactive elements, enabling reliable U–Th dating. A curve of Lake Lisan levels is constructed based on the stromatolite ages and cave elevations. The following points are noted: (1) Lake levels of −247 m relative to m.s.l., are recorded at ~75–72.5 ka; (2) relatively high lake levels above −220 m relative to m.s.l., are achieved at ~41.5 ka, and are still recorded at ~17 ka; (3) the peak level is −188 m relative to m.s.l., at ~35.5–29.5 ka. These results indicate lake stands up to 80 m higher than previously accepted, for large parts of the Lake Lisan time span. This difference is explained by tectonic subsidence of up to 2.2 m/ka within the Dead Sea depression since the latest Pleistocene. This subsidence rate is in the same order of magnitude with previously calculated subsidence rates for the Dead Sea depression [Begin, Z.B., Zilberman, E., 1997. Main Stages and Rate of the Relief Development in Israel. Geological Survey of Israel report, Jerusalem]. Unlike previous Lake Lisan level estimations, the new curve is measured at the relatively stable shoulders of the Dead Sea depression.

© 2008 Elsevier Ltd. All rights reserved.

1. Introduction

Caves occasionally act as "sediment traps" (Frumkin, 2001) sheltering sediments against weathering, chemical alteration, and/or recrystallization. Relict caves up to 200 m long are common in the Dead Sea area of Israel (Frumkin, 2000). The morphotectonic Dead Sea valley is Earth's deepest subaerial depression, bounded by the Dead Sea Fault Escarpment. A series of marine and lacustrine water bodies have been occupying the depression probably since the Late Miocene (Manspeizer, 1985; Horowitz, 1987; Steinitz and Bartov, 1991; Garfunkel and Horowitz, 1966; Avni, 1998; Frumkin, 2001), notably lakes Samra and Lisan of Pleistocene age and the Holocene Dead Sea. The character and present location of the Dead Sea basin sediments are related to two still ongoing processes:

(1) Vertical tectonic movements of the depression margins (Picard, 1943; Langozky, 1963; Niemi, 1997; Frumkin, 1997, 2001; Weinberger et al., 2007), as well as subsidence of its bottom (Reches and Hoexter, 1981; Eyal and Reches, 1983; Garfunkel, 1997; Steinitz and Bartov, 1991; Niemi and Ben-Avraham, 1997; Avni, 1998). Possible differential movements along the Fault Escarpment and across downfaulted blocks could create a complex tectonic history. Such movements may be assessed by correlating sediments of ancient water bodies along the escarpment, with sediments of known age within the basin (Frumkin, 2001).
(2) Climate-related lake level oscillations of the depression's water bodies (Manspeizer, 1985; Niemi, 1997). The lake levels are a gauge to the amounts of water supplied to the catchment area,

* Corresponding author. Tel.: +972 2 588 3352 or 3355; fax: +972 2 582 0549.
E-mail addresses: sorinl@012.net.il (S. Lisker), matthews@gsi.gov.il (M. Bar-Matthews), msamos@mscc.huji.ac.il (A. Frumkin).

0277-3791/$ – see front matter © 2008 Elsevier Ltd. All rights reserved.
doi:10.1016/j.quascirev.2008.10.015

so they are occasionally used as palaeo-climatic indicators (Picard, 1943; Neev and Hall, 1977; Begin et al., 1985; Frumkin, 1997; Frumkin et al., 2001; Stein, 2001). The cyclic nature of these levels and of the lake sediments, reflects the regional climate, i.e. alternations between wet and dry periods (Neev and Emery, 1967; Neev and Hall, 1977; Begin et al., 1985; Frumkin, 1997; Machlus et al., 2000; Stein, 2001; Bartov et al., 2002).

The lake levels thus reflect the water balance at the drainage area, and tectonic movements at the lake immediate vicinity. In the current research, U–Th dating of algal stromatolite sediments preserved in caves of the Fault Escarpment is used for palaeo-tectonic reconstruction of the area during the latest Pleistocene. Since algae are reliant upon sun-light in the upper water layer, stromatolite sediments are seen as proxies of the lake levels (Buchbinder et al., 1974; Buchbinder, 1981; Begin et al., 1985; Niemi, 1997).

Previous reconstructions of Late Pleistocene Lake Lisan stands were performed by means of sedimentological and stratigraphical analyses of the lake deposits: ancient lake shores were identified, beach and lacustrine sediments were correlated, and aragonite laminas of the lacustrine sediments were dated by U–Th and/or ^{14}C (Bartov, 1999; Bartov, 2004; Machlus et al., 2000; Bartov et al., 2002). Limited use of stromatolite ^{14}C dating was made by Neev and Emery (1967) and Begin et al. (1985). Their results do not match the above mentioned later reconstructions, and are not entirely reliable probably due to contamination by "young carbon" (Begin et al., 1985).

2. Geographical setting

The Fault Escarpment bounding the Dead Sea depression, and the deep canyons dissecting through it, are the most conspicuous morphologic features of the Dead Sea area of central eastern Israel. The studied caves are located along the northern section of the western Dead Sea shore (Fig. 1), between *En Gedi* and the famous archaeological cave area of *Qumran*, 0.5–4 km west of the current lake shore, in the lower parts of the Fault Escarpment at −310 to −188 m altitude relative to mean sea level (m.s.l.), i.e. ca 110 to 230 m above the current lake level (∼−420 m relative to m.s.l.).

3. Geological background

3.1. Tectonics

The morphotectonic depression of the Dead Sea started to form during the Late Miocene (Manspeizer, 1985; Horowitz, 1987; Steinitz and Bartov, 1991; Garfunkel, 1997; Avni, 1998; Frumkin, 2001), and continued into the Pleistocene (Avni, 1998) and Holocene (Reches and Hoexter, 1981; Eyal and Reches, 1983; Niemi and Ben-Avraham, 1997). The depression is bounded by normal and strike-slip faults (Garfunkel, 1981; Niemi and Ben-Avraham, 1997; Sagy et al., 2003; Ben-Avraham and Lazar, 2006; Shamir, 2006) (Fig. 2), forming the Dead Sea Fault Escarpment with a relief of up to 650 m above Dead Sea level.

The internal structure of the escarpment consists of steep (75–85°) tectonic faults with an overall throw of hundreds of meters (Agnon, 1981). Larger faults are buried under the depression's sedimentary fill, reaching a total throw of ∼6–12 km (Ben-Avraham and Lazar, 2006), downfaulting Cretaceous to Pleistocene units (Raz, 1983; Avni, 1998; Waldman, 2002). However, the escarpment is rather tectonically stable compared to the depression's inner parts, which have been affected by tectonic subsidence during the Pleistocene and Holocene (Raz, 1983; Ben-Avraham et al., 1993; Bowman, 1997; Avni, 1998; Waldman, 2002).

3.2. Bedrock stratigraphy

The bedrock stratigraphic column exposed in the Fault Escarpment and adjacent canyons, mainly comprises Cenomanian–Turonian carbonates of the Judea Group, reaching a thickness of about 600 m. The following formations have been described by Roth (1970a,b); Raz (1983, 1986); Mor (1987), and Mor and Burg (2000): Zafit (Lower–Upper Cenomanian; limestone, dolomite), Avnon (Upper Cenomanian; chalk, marl), Tamar (Upper Cenomanian–Lower Turonian; dolomite), Shivta (Lower–Upper Turonian; limestone, dolomite), Nezer (Upper Turonian; limestone, dolomite).

3.3. Water bodies and sediments within the Dead Sea basin

The ancient Mediterranean Sea penetrated the depression during the Late Miocene (Shaliv, 1991) and/or Pliocene (Stein et al., 1997), and deposited brackish sediments on its margins (Langozky, 1963; Shahar et al., 1966; Zak, 1967; Begin, 1975; Elron, 1980), while thick sequences of evaporites were deposited within the basin as the Sedom Formation of Late Miocene–Pliocene age (Zak, 1967; Bender, 1974; Horowitz, 1987; Shaliv, 1991; Steinitz and Bartov, 1991; Raab et al., 1997).

At Messinian times, the depression was disconnected from the open sea (Shaliv, 1991). A series of residual lakes have been occupying the depression during the Plio-Pleistocene and the Holocene, depositing evaporites, carbonates and clastic sediments (Stein, 2001). Post-depositional subsidence of the depression's floor resulted in a reversed stratigraphic sequence, which provide a relative time framework of the water bodies' sediments (Frumkin, 2001).

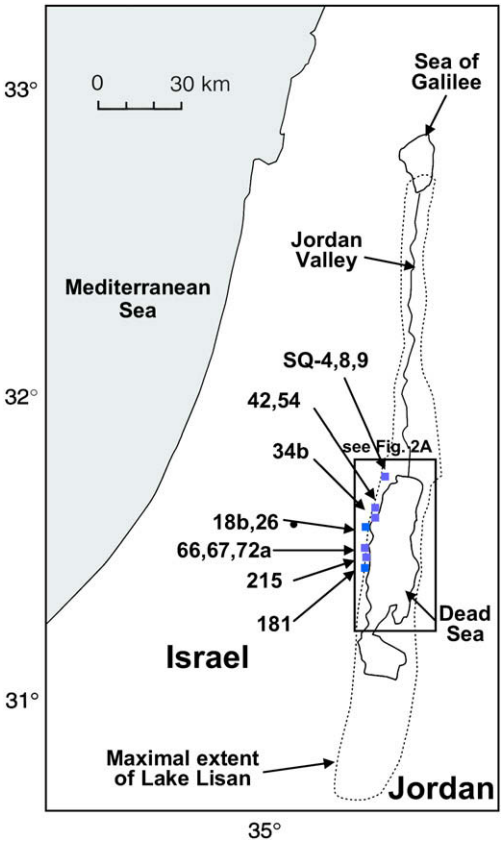


Fig. 1. Location map of research area and main caves with stromatolites.

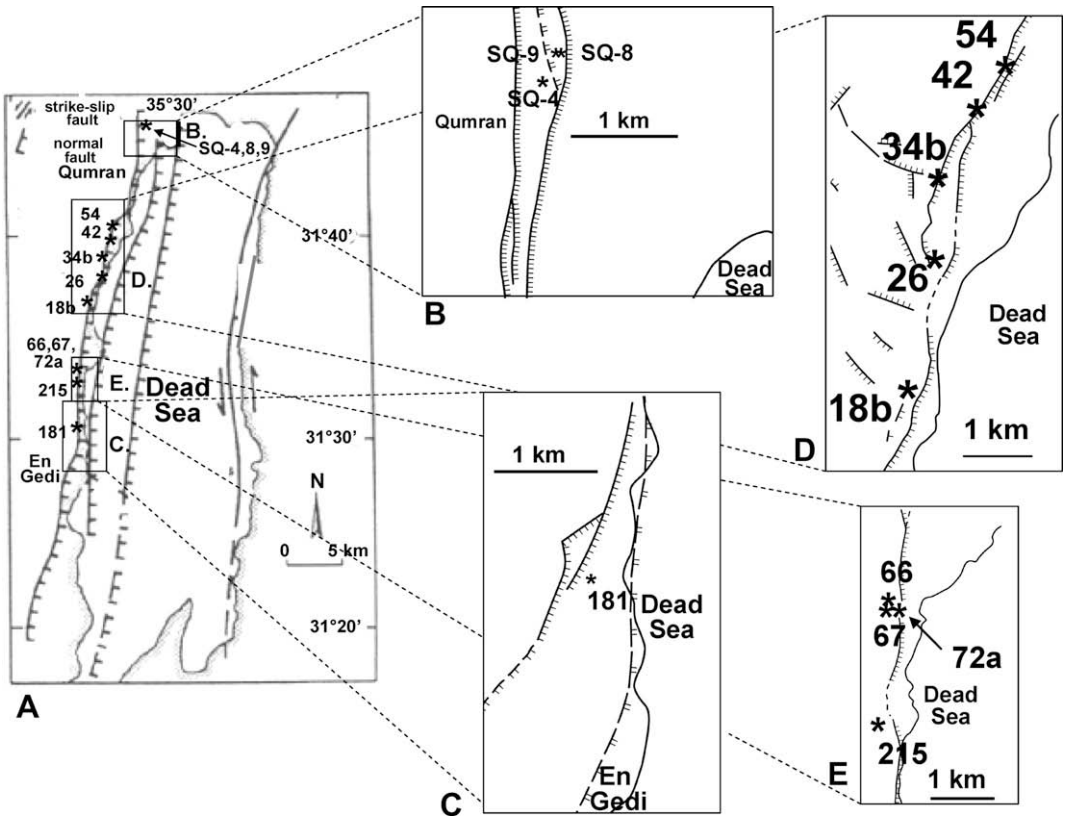


Fig. 2. Location of caves with stromatolites within the tectonic framework of the Dead Sea Fault Escarpment (its location roughly defined by the westernmost main faulting line). (A) Main research area (main faults after Niemi and Ben-Avraham, 1997). (B) Northern part of research area (Qumran area) (main faults after Roth, 1970b). (C) Southern part of research area (En Gedi area) (main faults after Raz, 1986). (D, E) Central part of research area (main faults after Mor and Burg, 2000). See text for details.

Darga Conglomerate of Plio-Pleistocene age, with a thickness of 10–15 m, discontinuously crops out along the northern segment of the Fault Escarpment, at altitudes of −390 to −70 m relative to m.s.l., unconformably overlying Zafit and Tamar Formations, and occasionally dissected by faults (Roth, 1970a; Raz, 1983; Mor, 1987). The conglomerate was described as "debris flows" or "estuarine deposits" (Manspeizer, 1978, 1985; Raz, 1983; Mor, 1987) deposited on the lake shore (Roth, 1970a), mainly containing angular limestone, dolomite and chert pebbles derived from the Judea Group, cemented by authigenic carbonate (Mor, 1987) precipitated by springwater (Roth, 1970a; Garfunkel, 1978).

Samra Formation of Pleistocene age mainly containing marls, sandstones, limestones, evaporites and conglomerates, was deposited within Lake Samra (Picard, 1931, 1943; Bentor and Vroman, 1957; Kaufman et al., 1992; Stein, 2001; Waldmann, 2002), between ~140 and 75 ka (MIS-5) (Waldmann et al., 2007). Lake Samra levels fluctuated between −400 and −70 m relative to m.s.l.

Lisan Formation of Late Pleistocene age unconformably overlies the Samra Formation, typically containing alternations of detritic and aragonite laminas, as well as conglomerates, clays and evaporites (Begin et al., 1974, 1980; Niemi, 1997; Bartov et al., 2002). In the Dead Sea area, the formation is well dated by U–Th and radiocarbon to the last Glacial (MIS-4–2: Martinson et al., 1987), ca 70–15 ka (Begin et al., 1974, 1980; Sneh, 1979; Kaufman et al., 1992; Machlus et al., 2000; Schramm et al., 2000; Stein, 2001; Bartov et al., 2002).

Lake Lisan was hypersaline, though less so than the Dead Sea (Stein et al., 1997). Its stands were reconstructed by various authors, among others: Machlus et al., 2000; Schramm et al., 2000; Stein, 2001; Bartov et al., 2002; Bartov, 2004; Haase-Schramm et al., 2004. The lake levels fluctuated between a minimum of −340 m and a maximum of −180 to −150 m relative to m.s.l. (Neev and Emery, 1967; Elron, 1980; Begin et al., 1980, 1985; Bowman and Gross, 1992; Stein et al., 1997; Machlus et al., 2000; Stein, 2001; Bartov et al., 2002), or even higher at −130 m (Plakht et al., 2002). At its peak levels, Lake Lisan filled the depression from the current Sea of Galilee in the north to ca. 30 km south of the current Dead Sea (Fig. 1) (Niemi, 1997; Stein, 2001; Bartov 2004; Haase-Schramm et al., 2004), penetrating as fjord-like water tongues into the deep canyons of the Fault Escarpment (Bartov et al., 2002; Plakht et al., 2002). Several studies, reviewed by Enzel et al. (2008), suggest that the lake levels reflect the regional climate in the Eastern Mediterranean.

The Lisan Formation deposited within the lake, is divided into three members: (1) Lower Member dated 70–55 ka, mainly composed of alternations between aragonite and detritic laminas, and gypsum layers; (2) Middle Member dated 55–35 ka, mainly containing clastic layers; (3) Upper Member dated 35–15 ka, mainly containing alternations between aragonite and detritic laminas, with a gypsum layer. Since its peak level at 26–25 ka, the lake has been almost continuously shrinking until almost complete desiccation at 12–11 ka (Bentor and Vroman, 1960; Neev and Emery, 1967; Begin et al., 1985). The Lisan sediments are mainly exposed along the Fault Escarpment, and at the openings of the canyons dissecting the escarpment. The original aragonite of the sediments is preserved due to the dry climate of the area.

The basin was again inundated, this time by the Dead Sea, at 10,300–9500 years BP. During most of the Holocene, the lake level was at ca −400 m, with small oscillations (Frumkin, 1997; Kadan, 1997; Frumkin et al., 2001; Stein, 2001; Bookman (Ken-tor) et al., 2004; Migowski et al., 2006), prior to an anthropogenic and still ongoing drop to ca −420 m relative to m.s.l., during the last few decades.

The Dead Sea sediments include lacustrine and fluviatile facies (Neev and Emery, 1967; Neev and Hall, 1977; Stein, 2001): aragonite–detritic laminar alternations similar to those of the Lisan Formation, clastics, and evaporites. A limited array of primitive micro-organisms is present in today's Dead Sea waters (Buchalo et al., 1998).

3.4. Stromatolites of the Dead Sea basin

Algal communities flourished in Lake Lisan and even affected the chemistry of its waters (Kolodny et al., 2005). Stromatolite sediments associated with Lake Lisan are reported by Bentor and Vroman (1960), Neev and Langozky (1961), Zak (1967), Neev and Emery (1967), Buchbinder et al. (1974), Begin (1975), Buchbinder (1981), Begin et al. (1985), and Niemi (1997). According to these authors, Lake Lisan stromatolites are characterized by aragonite mineralogy, high porosity, laminar layering, and microstructure of spheroids and/or peloids. According to Pia (1933, p. 65), stromatolite-forming algae along the Dead Sea shore are of the species Oocardium stratum. The original mineralogy of stromatolite deposits is generally dictated by the chemistry of the water body, and is similar to other sin-depositional carbonate sediments within the basin. Accordingly, the Lake Lisan stromatolites are mainly composed of aragonite, and are similar to other Lisan sediments (Buchbinder, 1981). However, the Lisan stromatolites occasionally undergo recrystallization to low-Mg calcite, though on a limited scale due to the region's aridity (Buchbinder et al., 1974).

In addition to Lake Lisan, stromatolites of Lake Samra (Waldmann, 2002) and Holocene stromatolites (Druckman, 1981) were also reported in the Dead Sea area.

4. Methods

4.1. Field work

Oblique air-photos were shot at 45° relative to the horizon and according to the topography of the Fault Escarpment. They were used for identification of cave openings. A cave survey on foot was undertaken along the escarpment cliffs. The cave locations (coordinates) and altitudes were measured using a Garmin eTrex Summit GPS, with a position accuracy of 15 m (49 ft) and altimeter accuracy of ±10 ft and resolution of 1 ft. Stromatolite sequences encountered within the caves, were sampled along measured stratigraphic sections, for further laboratory analyses.

4.2. Laboratory methods

Samples were treated prior to analyses at the laboratories of the Department of Geography of the Hebrew University of Jerusalem.

Thin-sections were prepared at the laboratories of the Earth Sciences Institute of the Hebrew University of Jerusalem, and the Geology Department of the Ben-Gurion University of Beer-Sheba, Israel. They were examined using a Nikon polarizing microscope. Characteristic textures and structures were checked out and identified, and the mineralogy was initially defined. An attempt was made to identify recrystallization and/or chemical alteration, in order to verify system closure regarding radioactive elements, enabling further U–Th dating.

XRD mineralogy analyses were performed at the Unit for Nanoscopic Characterization of the Hebrew University, with a Bruker AXS D8 Advance diffractometer, and at the

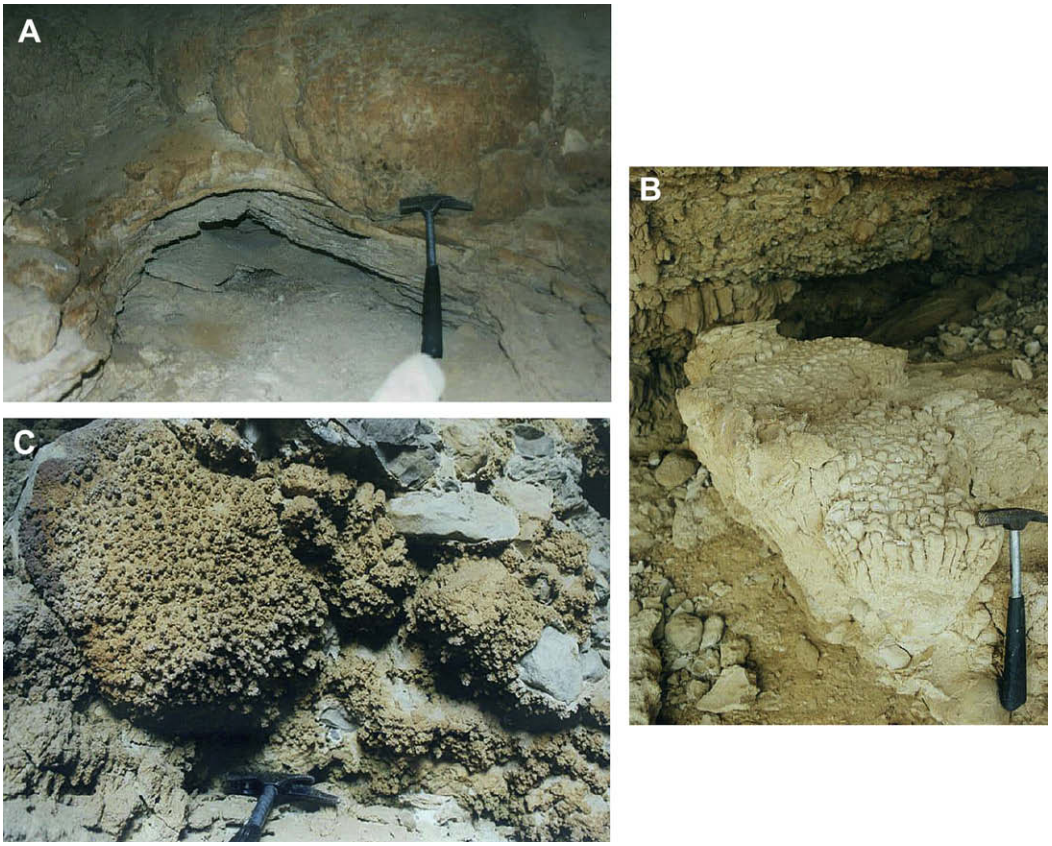


Fig. 3. (A) Dome-shaped (hemispheroidal) stromatolite of Cave 66. (B) Laterally-linked columnar stromatolites on floor of Cave 215. (C) "Coralloid" stromatolites on walls of Cave 67.

laboratories of the Geological Survey of Israel, with a Phillips PW 1830/3710 diffractometer. Preservation of the stromatolites' original aragonite mineralogy, served also as an indicator for closed system.

U–Th dating analyses were performed at the geochemistry laboratories of the Geological Survey of Israel. The dating analyses were performed on laminas in stratigraphical sequence, of sampled stromatolite sections from 11 caves, ranging in altitude between −292 m (Cave SQ-8) to −188 m (Cave 66) relative to m.s.l. Dating methods based on the ^{230}Th–^{234}U system are often used on carbonate sediments, and were discussed, among others, by Schwarcz (1986) and Kaufman et al. (1998). Samples were dated by Multi Collector Inductive Coupled Plasma Mass Spectrometry (MC-ICP-MS), using a Nu Instruments spectrometer. The MC-ICP-MS configuration for U–Th dating analyses is described by Vaks et al. (2006). Sample preparation for dating analyses, included separation of detritus from the authigenic carbonate (Bar-Matthews et al., 1997), and separation of U and Th from the carbonate, separation between U and Th by ion exchange techniques, and chromatographic separation (Vaks et al., 2006). The spike used was ^{236}U–^{229}Th.

Corrections for detritic ^{230}Th were performed for stromatolite samples with ^{230}Th/^{232}Th < 100 (Kaufman et al., 1998; Vaks et al., 2006), assuming the ^{232}Th/^{238}U ratio of Lisan Formation aragonite, i.e. 0.85 (Haase-Schramm et al., 2004). Ages of samples with evidence for recrystallization (i.e. with predominantly calcite mineralogy) and samples containing very high detritus content (i.e. with ^{230}Th/^{232}Th < 10) were discarded.

5. Results

5.1. Stromatolites in caves of the Dead Sea Fault Escarpment

Stromatolites were identified in caves along the Fault Escarpment (Fig. 1), from the entrance area down to ca. 10 m inside the cave. The stromatolite caves are located between −310 to −188 m altitude relative to m.s.l., within the Plio-Pleistocene Darga Conglomerate, and Tamar and Zafit carbonate formations of Cenomanian age.

5.1.1. Morphology

Typical stromatolite morphologies as defined by the classification of Logan et al. (1964), were encountered in the caves: "dome-shaped" (hemispheroidal) and "club-shaped" (columnar) stromatolites (Fig. 3A,B), with laminar or wavy-laminar internal structure. Both types usually occur as clusters of closely-packed laterally-linked individuals, often as crusts covering the cave walls. Other types were occasionally encountered, including "coralloids" (Fig. 3C), laminar crusts, and porous formations of irregular shape often with "spongy" appearance. Various stromatolite types were often encountered together in the same cave, as simple separate structures, or composite structures with internal stratigraphy.

5.1.2. Petrography and mineralogy

Characteristic stromatolite textures and structures (Monty, 1981) were observed in thin-sections: aragonite spheroids up to

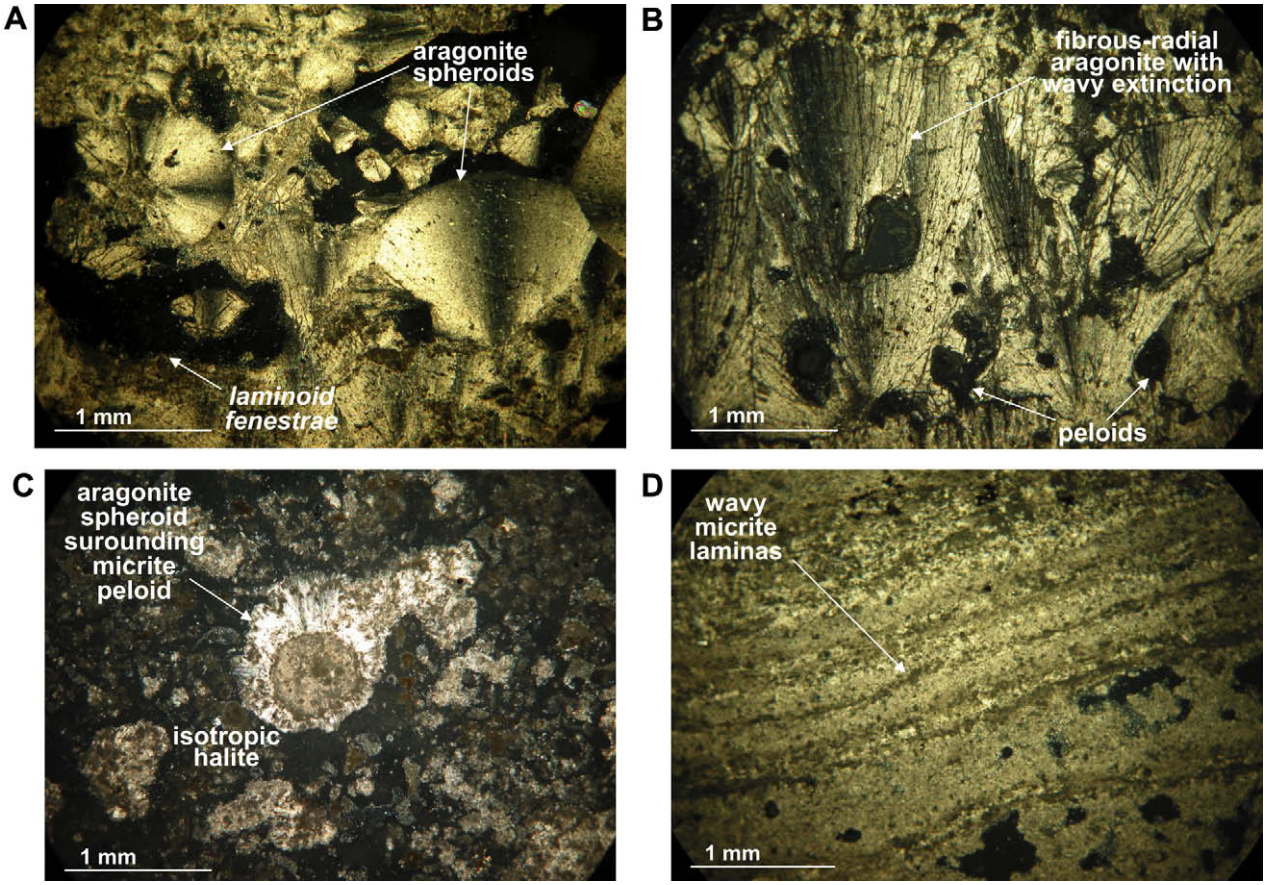


Fig. 4. (A) Thin-section (polarized light) of stromatolite sample from Cave 26, containing aragonite spheroids and laminoid fenestrae. (B) Thin-section (polarized light) of stromatolite sample from Cave 36b, containing fibrous-radial aragonite crystals with wavy extinction, and peloids. (C) Thin-section (polarized light) of stromatolite sample from Cave 66, containing isotropic halite, and aragonite spheroid surrounding micrite peloid; (D) Thin-section (polarized light) of stromatolite sample from Cave 26, containing wavy micrite laminas.

Table 1
U–Th dating results of stromatolite sections from caves of the Dead Sea Fault Escarpment.

Cave	Altitude (m relative to a.s.l.)	Sample	Height of sample above base of section (cm)	Age (ka; uncorr.)	2σ	Age (ka; corr. $^{232}Th/^{238}U = 0.85$)	^{238}U (ppm)	$^{234}U/^{238}U$ (corr. $^{232}Th/^{238}U = 0.85$)	$^{230}Th/^{234}U$ (corr. $^{232}Th/^{238}U = 0.85$)	$^{230}Th/^{232}Th$	Mineralogy (main phases)
66	−188	S-66 IV-K	60	32.3	0.29	30.4	2.2	1.5	0.2473	53.528	Aragonite, Halite, Quartz
		S-66 IV-J	54.5	31.1	0.24	29.3	3.7	1.4965	0.23944	54.725	Aragonite, Halite
		S-66 IV-I	50-54	31.5	0.20	–	4.3	1.4865	0.25501	127.92	Aragonite
		S-66 IV-H	50	33.6	0.26	–	3.6	1.4884	0.27012	111.01	Aragonite
		S-66 IV-F upp.	36	33.7	0.24	–	4.1	1.4878	0.27048	137.98	Aragonite
		S-66 IV-F low.	31	37	0.21	35.6	4.2	1.4785	0.2834	77.185	Aragonite
215	−198	S-215 D-IV	50	30.7	0.33	29	2.9	1.4967	0.2374	57.497	Aragonite
		S-215 D-III	30-35	29.7	0.43	28.1	3.8	1.4945	0.2307	59.607	Aragonite
		S-215 D-II	25-30	33.8	0.21	31.9	3.6	1.4965	0.2581	57.206	Aragonite
		S-215 D-I	0-5	35.3	0.16	31.8	3.9	1.4931	0.2574	31.869	Aragonite
		S-215 D-I upp.	5	34.2	0.18	26.1	4.4	1.5405	0.21609	13.674	Aragonite
		S-215 D-I low.	0	34.9	0.27	32.2	3.9	1.4881	0.26011	41.318	Aragonite
		S-215 I	[a]	35.7	0.22	29.5	3.3	1.5103	0.2406	18.262	Aragonite, Halite
34b	−201	S-34b I	[a]	31.5	0.21	30.1	3.8	1.4878	0.2451	69.378	Aragonite
		S-34b II	[a]	32.8	0.18	–	4.6	1.4838	0.26398	276.96	Aragonite, Halite, Gypsum
		S-34b Y-VI	12	22.9	0.54	17	2.5	1.5057	0.14620	13.248	Aragonite, Gypsum
		S-34b Y-IV	5	42	0.52	30.6	3.1	1.4859	0.24865	11.689	Aragonite
		S-34b Y-III	2	49.4	0.46	38.6	2.7	1.4541	0.30380	14.039	Aragonite
		S-34b Y-II	1	34.7	0.47	28.9	2.7	1.4987	0.23646	19.270	Aragonite
		S-34b Y-I	0	42.7	0.49	34.4	3.1	1.3617	0.27488	16.12	Aragonite
42	−213	S-42 A-V	9	29.6	0.68	–	3.1	1.47800	0.24121	35.874	Aragonite
		S-42 A-III	5	30.9	0.20	–	3.6	1.48255	0.25090	174.22	Aragonite
		S-42 A-II	2.5	33.9	0.20	–	5.8	1.4906	0.27219	232.04	Aragonite
		S-42 A-I	0	34.1	1.17	–	4.4	1.49907	0.27347	70.49	Aragonite
		S-42 II	[a]	32	0.19	28.296	4.2	1.5002	0.2321	27.943	Aragonite
181	−214	S-181 C	8-9	31.9	0.57	–	3.9	1.48587	0.25763	35.33	Aragonite
		S-181 B	5	30.7	0.56	26.6	3.9	1.5150	0.21953	24	Aragonite
		S-181 A	0-3	33.7	0.61	–	3	1.47546	0.26518	32.36	Aragonite
18b	−219	S-18b III	10	53.1	0.72	40.2	3.9	1.4336	0.31450	12.532	Aragonite, Calcite, Halite
		S-18b II	5	45.1	1.55	39.3	3.9	1.4305	0.30821	23.64	Aragonite, Calcite
		S-18b I	2	50.5	1.42	41.5	3	1.4502	0.32296	16.90	Halite
54	−234	S-54 F-1	–	33.4	0.43	–	5.1	1.49053	0.26844	103.04	Aragonite
		S-54 IV	–	35.2	0.73	–	4.6	1.48074	0.28067	64.677	Aragonite
		S-54 III	70-85	33.1	0.32	–	5.7	1.49299	0.26629	147.15	Aragonite
		S-54 II	60	35.4	0.41	–	4.2	1.47455	0.28238	63.567	Aragonite
		S-54 0	20	37	0.26	–	4.5	1.4748	0.29317	210.76	Aragonite
		S-54 00	0	43.2	0.77	–	3.5	1.47438	0.33383	47.94	Aragonite
		S-54 VI	[a]	45.2	0.38	–	3.9	1.47831	0.34666	387.49	Aragonite
SQ-4	−243	SQ-4 B-III	35	32.9	0.24	30.5	3.3	1.4864	0.24793	43.65	Aragonite
		SQ-4 B-II	30	34.7	0.90	29.8	2.9	1.5122	0.24300	22.71	Aragonite
		SQ-4 III	30	34.5	0.19	32.6	5.2	1.5013	0.2632	59.174	Aragonite
		SQ-4 B-I	25	40.5	0.34	33	3.4	1.5182	0.26601	17.026	Aragonite
		SQ-4 IV	15	36.8	0.25	29.1	2.3	1.5229	0.23769	15.261	Aragonite
72a	−247	S-72 A-II	20	77.9	0.49	72.5	3.5	1.4635	0.50160	37.330	Aragonite
		S-72 A-I	0	79.5	0.51	74.9	3.9	1.4886	0.51410	43.958	Aragonite
SQ-9	−262	SQ-9 C	70	47.7	0.43	41.9	2.6	1.5261	0.32586	24.630	Aragonite
		SQ-9 B	35	65.8	0.55	59.2	2.5	1.4712	0.43047	27.68	Aragonite
		SQ-9 A	0	71.1	1.25	67.4	2.7	1.5068	0.47595	50.40	Aragonite
		SQ-9 II	[a]	53.363	1.03	–	3.5	1.47267	0.39686	62.01	Aragonite
SQ-8	−292	SQ-8 C	30	52.7	0.43	46.9	2.6	1.4925	0.35777	26.47	Aragonite
		SQ-8 B	15	57.5	0.47	54.8	2.3	1.5278	0.40631	62.01	Aragonite
		SQ-8 A	0	54.2	0.62	50.3	2.2	1.5330	0.37899	39.33	Aragonite

[a] Sample not part of stratigraphic section.

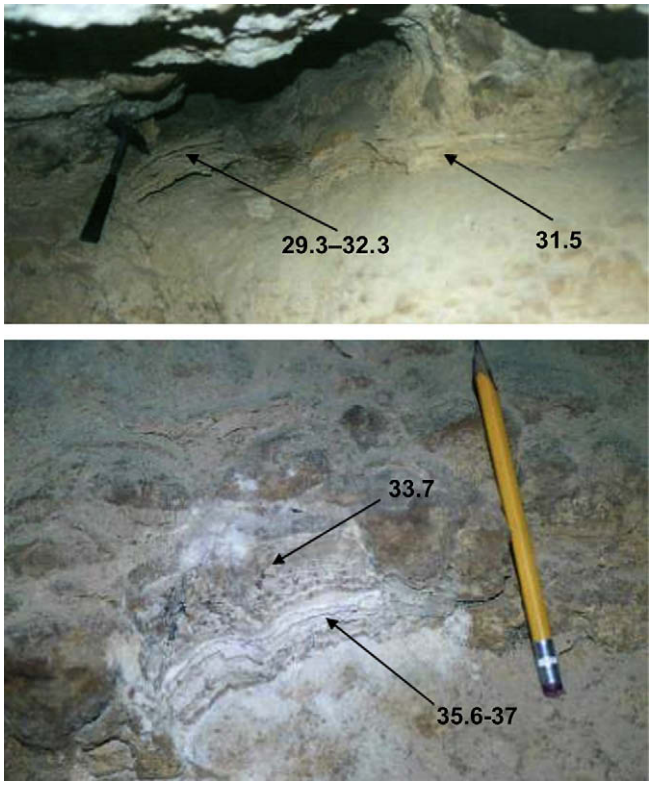


Fig. 5. Dated stromatolite section of Cave 66. Here and in Figs. 6, 7: Ages in ka; within each pair of results: the higher value indicates the uncorrected age; the lower value indicates the age corrected for detrital ^{230}Th using a ^{233}Th/^{238}U value of 0.85 (Haase-Schramm et al., 2004); a single value indicates an age not requesting correction due to low detritus content.

1 mm diameter (Fig. 4A); fibrous-radial aragonite crystals up to 1.3 mm long with wavy extinction (Fig. 4B), occasionally concentric, often forming laminas or filling voids; micrite; laminoid fenestrae voids (Fig. 4A); peloids (Fig. 4B,C); evaporites (Fig. 4C); wavy-laminar alternations of light- and dark-colored laminas up to a few mm thick (Fig. 4D).

XRD analyses indicate that the stromatolite samples are usually composed of aragonite as the main mineral (Table 1). Evaporites (halite, gypsum, anhydrites) are often present as main and/or secondary minerals. In few cases, secondary calcite partially or totally replaces the original aragonite.

5.2. U–Th ages of stromatolites

Three of the dated stromatolite sections are shown in Figs. 5–7. The ages of the stromatolites are shown in Table 1. The relative altitudes and locations along the Fault Escarpment of caves with dated stromatolites are shown in Fig. 8. The following points are noted:

(1) The (corrected) stromatolite ages range between ~75 ka (Cave 72a at −247 m relative to m.s.l.) to ~17 ka (Cave 34b at −201 m relative to m.s.l.). This range of ages covers the time span of Lake Lisan (Begin et al., 1974, 1980; Kaufman et al., 1992; Machlus et al., 2000; Schramm et al., 2000; Stein, 2001; Bartov et al., 2002).
(2) The oldest ages, i.e ~75–72.5 ka (Cave 72a at −247 m relative to m.s.l.) and ~67.5 ka (Cave SQ-9 at −262 m relative to m.s.l.), reach the Lake Samra to Lake Lisan transition (90–70 ka: Waldmann, 2002), i.e. MIS-5–4 transition (Martinson et al., 1987).

The ages are usually in accordance with the stratigraphic order of the laminas. However, a few exceptions are noted (Table 1). In

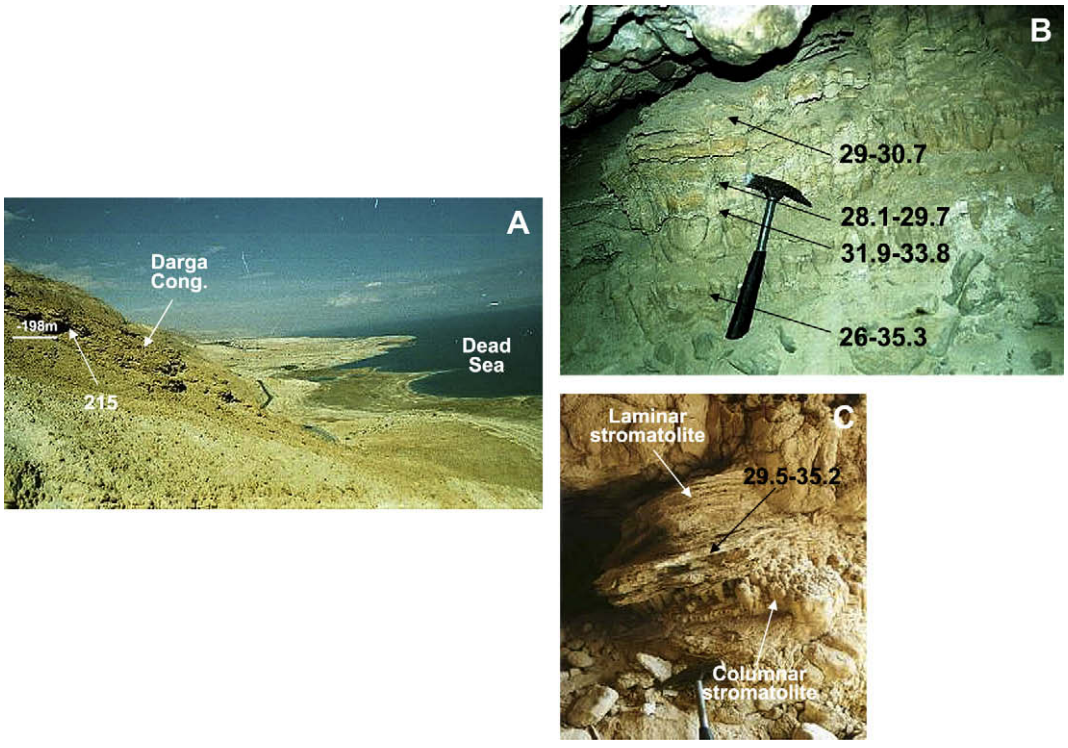


Fig. 6. Cave 215. (A) Cave opening within layers of Darga Conglomerate. (B) Dated stromatolite section. (C) Dated stromatolite outcrop.

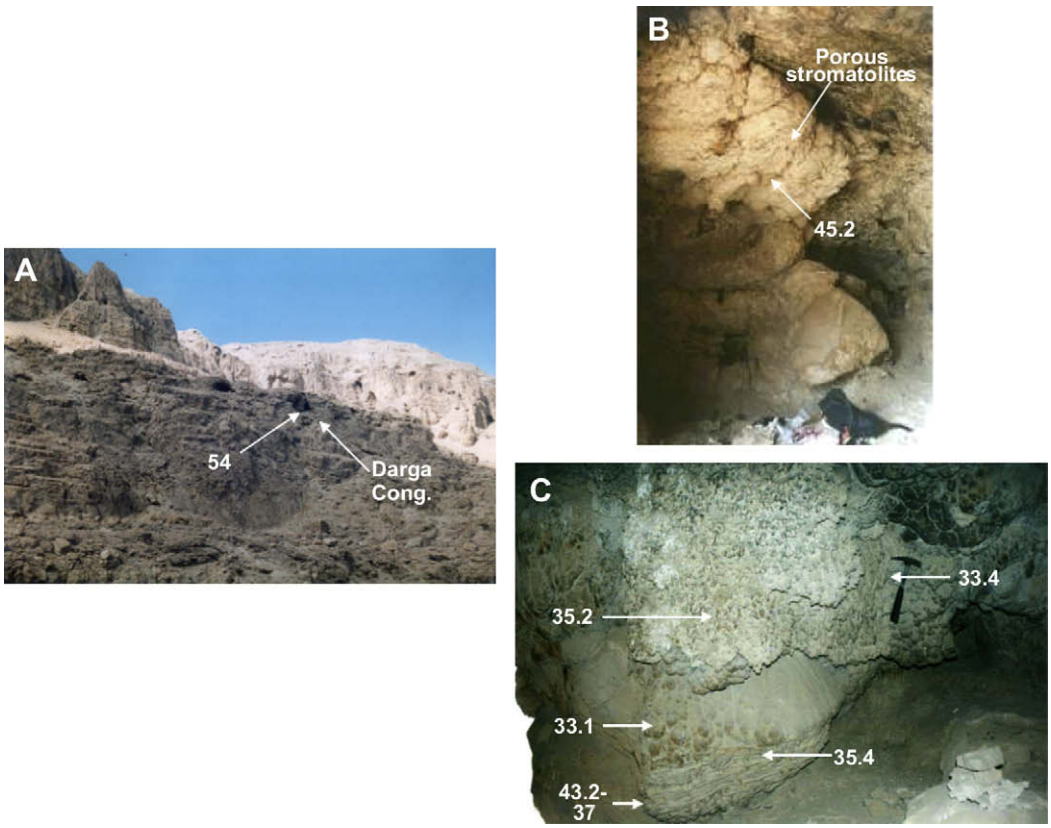


Fig. 7. Cave 54. (A) Cave opening within layers of Darga Conglomerate. (B) Dated stromatolite outcrop on cave ceiling. (C) Dated stromatolite section.

Caves 215 (Sample S-215 D-I upper), 34b (Samples S-34b Y-II, S-34b Y-III), 181 (Sample S-181B), 54 (Sample S-54 III), SQ-4 (Sample SQ-4 IV), and SQ-8 (Sample SQ-8 B), there are deviations up to a few ka (Table 1). Most of these samples have low $^{230}Th/^{232}Th$ ratios, i.e. between 13.7 and 24. These suggest high amounts of detritic Th which possibly are the cause for the deviations from the stratigraphic order. The required corrections apparently further increased the deviations (Table 1). However, age corrections of aragonite Lisan sediments can also significantly increase the error range of the results up to one order of magnitude, as shown by Haase-Schramm et al. (2004), thus actually reducing the deviations. In any case, the ages of the above samples are still consistent with the age range of the relevant sections (Table 1).

Three samples from Cave 66 and three from Cave SQ-5 yielded anomalous $^{230}Th/^{234}U$ ratios or unreliable ages, with calcite substituting aragonite as the main mineralogical phase, probably due to recrystallization. A sample from Cave 72a yielded an unreliable age due to very high contamination by detritus, as indicated by a low $^{230}Th/^{232}Th$ ratio of 6.6. These samples were not used for lake level reconstruction.

6. Discussion

6.1. Comparison with other stromatolites from the Dead Sea area

Wavy-laminar stromatolites were previously documented in the Dead Sea area (Neev and Langozky, 1961; Buchbinder et al., 1974; Druckman, 1981; Buchbinder, 1981), though not in caves. Holocene stromatolites with laminar dome structures are reported along the Dead Sea shore by Druckman (1981), though no laterally-linked dome-shaped or club-shaped Lake Lisan stromatolites were documented prior to this study. Other stromatolite types encountered

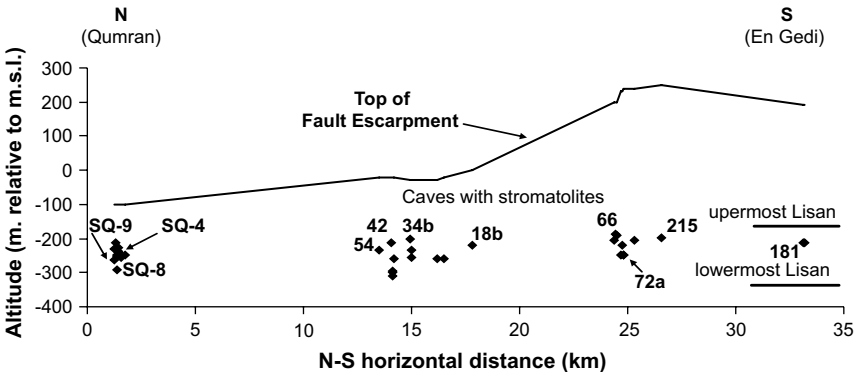


Fig. 8. Relative altitude of caves with stromatolites along the Fault Escarpment between Qumran and En Gedi. For U–Th ages of the stromatolites, see Table 1.

within the caves, e.g. crusts on cave walls, formations of irregular shape etc., are also reported in the area (Neev and Langozky, 1961). The porous "spongy" appearance often with laminoid fenestrae voids, is a common characteristic of Lake Lisan stromatolites (Neev and Langozky, 1961; Buchbinder et al., 1974), the voids being left by decay of algal organic matter.

Composite stromatolite formations reflect changes in the conditions of the depositional environment, such as lake level fluctuations or runoff and alluvium input (Logan et al., 1964); both are common throughout Lake Lisan's sedimentary record.

Pelloids and pelloidic aragonite laminas, which are widespread among the cave stromatolites, are also common among Lake Lisan stromatolites (Buchbinder et al., 1974), and among Holocene stromatolites in the area (Druckman, 1981).

According to Buchbinder et al. (1974) and Buchbinder (1981), stromatolites of Lake Lisan are composed of aragonite as the main mineral phase, often with microstructures of aragonite spheroids representing recrystallized blue-green algae cells, void-filling biochemically-precipitated fibrous aragonite crystals, or concentric or radial-concentric aragonite crystals with wavy extinction. All these features are similar to those encountered in the cave stromatolites.

The above comparison clearly indicates that the studied stromatolites were deposited in Lake Lisan.

6.2. Reconstruction of Lake Lisan levels based on stromatolites

The stromatolite ages can be used for reconstruction of Lake Lisan stands, following two main working assumptions:

(a) The algae required sunlight for photosynthesis, thus they could only inhabit a shallow-water environment, enabling them to be used as a lake level gauge (Buchbinder et al., 1974; Buchbinder, 1981; Begin et al., 1985; Niemi, 1997). However, stromatolite occurrences down to ca. 10 m inside some caves, suggest algae's ability to withstand various light intensities.

(b) A "closed system" was maintained since the stromatolite deposition, based on the fact that the cave environment is sheltered from rain and runoff. Exposure to precipitation may lead to removing of soluble isotopes, e.g. U, hence lowering the analyses' reliability. This is particular acute while dealing with porous materials such as stromatolites, or aragonite sediments as those of Lake Lisan which are prone to recrystallization to calcite. The caves are dry, no evidence of water penetration since Lisan times has been noted, so they are considered adequate for preserving the sediments in their original state, with very little or no leaching or addition of U to the system. Thus we can assume that the U–Th ages represent the original age of the stromatolites. This assumption is further supported by preservation of the original aragonite mineralogy (Table 1), and the original stromatolite structures (Fig. 3) and microstructures (Fig. 4A–D).

Fig. 9 presents the stromatolite altitudes vs their ages. A curve was drawn by linking points of uppermost altitude among stromatolite samples of similar age. Based on the above assumptions, the curve shows the Lake Lisan levels between ~75 and 17 ka.

Some stromatolite ages appear under the lake level curve (Fig. 9), representing altitude differences of tens of meters between caves with stromatolites of similar age. Possible explanations are considered:

(1) Algae growing under the water level sensu stricto, while still confined to the photic upper level of the water body, due to their ability to withstand a spectrum of luminosities, as evidenced by stromatolite occurrences within the semi-obscure cave environment.

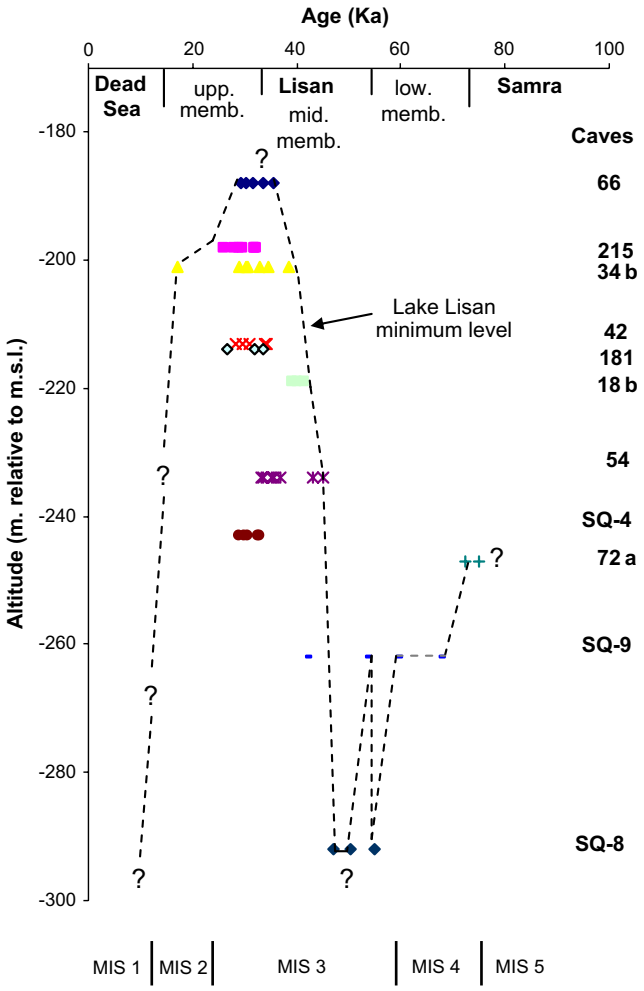


Fig. 9. Lake Lisan level curve according to altitudes and U–Th ages of stromatolites from caves of the Fault Escarpment. Marine Isotopic Stages (MIS) after Martinson et al., 1987.

(2) Lake level oscillations on a centennial to millennial scale: The 75–17 ka time interval is punctuated by cold Heinrich Events at 38, 31 and 24 ka, and intercalating warm Dansgaard–Oechger events. Bar-Matthews et al. (1999), Bartov et al. (2003), Haase-Schramm et al. (2004), and Bartov et al. (2006), argue that the amount of rainfall in the Eastern Mediterranean region was influenced by these events which would result in rapid lake level oscillations. These are probably not detected by the presented lake level curve, and thus apparently overlap.

(3) Local tectonic movements within the Fault Escarpment. The escarpment is stable relative to the inner parts of the Dead Sea depression (see Section 6.3 below), but local subsidence could have occasionally downlifted caves with stromatolites from their original location. A complex network of normal faults and intermediate tectonic blocks occurs along the whole length of the Dead Sea Fault Escarpment (see mapping of Roth, 1970b; Raz, 1986; and Mor and Borg, 2000). Some of the caves are located within such blocks (Fig. 2A–E), most notably lowermost Caves SQ-8 and SQ-9 located within a subsided block bounded by normal faults (Fig. 2B; see also Section 6.3 below), and Caves 18b, 34b, 42 and 54, located amidst a complex network of normal faults (Fig. 2D).

Our data do not allow one to distinguish between the above scenarios, and a combination of them is most likely. The lake level curve based on stromatolites (Fig. 9) should be thus regarded as a minimum Lake Lisan level pointer at any given time: the lake level

must have at least reached the curve/cave altitude in order to deposit stromatolites at that time.

It is clear from the lake level curve that:

(1) A stand of at least −247 m relative to m.s.l. was already achieved at ~75–72.5 ka (Cave 72a). This age correlates with Lake Samra to Lake Lisan transition (Waldman, 2002).
(2) Relatively high Lake Lisan stands (represented by stromatolites from Cave 66 at −188 m, Cave 215 at −198 m, Cave 34b at −201 m, Cave 42 at −213 m, Cave 181 at −214 m, and Cave 18b at −219 m, relative to m.s.l.), were already achieved at ~41.5 ka (Cave 18b), and persisted until ~17 ka (Cave 34b); these ages correlate with the later part of the Middle Member and the Upper Member of the Lisan Formation (Begin et al., 1974, 1980; Kaufman et al., 1992; Machlus et al., 2000; Schramm et al., 2000; Stein, 2001; Bartov et al., 2002). As Lake Lisan levels are indicative of palaeo-climate at the lake catchment area (Picard, 1943; Neev and Hall, 1977; Begin et al., 1985; Frumkin, 1997; Frumkin et al., 2001; Stein, 2001), even reflecting the regional climate in the Eastern Mediterranean (Enzel et al., 2008), these stands suggest relatively moist climate for the above time interval.
(3) The highest stromatolite level of −188 m relative to m.s.l., was already achieved at ~35.5–29.5 ka (Cave 66).

6.3. Tectonic implications of Lake Lisan levels according to stromatolites

The curve shown in Fig. 9 generally points at Lake Lisan stands between −292 to −188 m relative to m.s.l., within the range of previous reconstructions, i.e. −340 to −150 m relative to m.s.l. (Machlus et al., 2000; Bartov et al., 2002; Waldmann, 2002; Bartov, 2004).

Fig. 10 displays a comparison between the lake levels reconstructed in this study, and the lake level reconstruction of Bartov (2004) mainly based on deposits of the depression fill. This comparison shows that relatively high lake stands were already achieved at ~41.5 ka, i.e. ~15 ka earlier than previously assumed. We suggest that the apparent differences between the two lake level reconstructions are due to rift valley tectonics since the latest Pleistocene.

Normal faults bounding tectonic blocks of the Fault Escarpment are the most conspicuous structural element of the depression's margins (Fig. 2A), reaching a vertical throw of up to 500 m (Agnon, 1981). Yet larger-throw faults are buried under the depression's sedimentary fill. Previous lake level reconstructions (e.g. Machlus et al., 2000; Bartov et al., 2002; Waldmann, 2002; Bartov, 2004) were usually performed by dating samples of the depression fill, belonging to outcrops deposited upon subsided blocks east of the Fault Escarpment. These sites have been affected by tectonic subsidence of the Dead Sea depression during the Pleistocene and Holocene (Raz, 1983; Ben-Avraham et al., 1993; Bowman, 1997; Avni, 1998; Waldman, 2002), yet lake levels obtained in previous studies were usually not corrected for this subsidence, though an attempt was made by Bartov, 2004 (figure 32). Since the currently dated stromatolites were sampled on the relatively stable Fault Escarpment, west of the main faults (Fig. 2A), it is suggested that the stromatolite levels more closely represent the original lake stands.

The main conclusion of the comparison displayed in Fig. 10 is: between ~45 and 17 ka the stromatolite levels are tens of meters higher than previously calculated lake levels, up to 80 m at 35.6 ka (Cave 66). This difference can be quantitatively explained by up to 80 m/35.6 ka subsidence of intermediate blocks within the depression, i.e. up to 2.2 m/ka subsidence rate relative to the escarpment west of the main faulting zone.

Lisan outcrops dated 28–22 ka are exposed on the Fault Escarpment at Mount Izrach, 210–160 m below m.s.l. (Bartov, 2004, figure 17 and table 2). These levels are similar to the current results

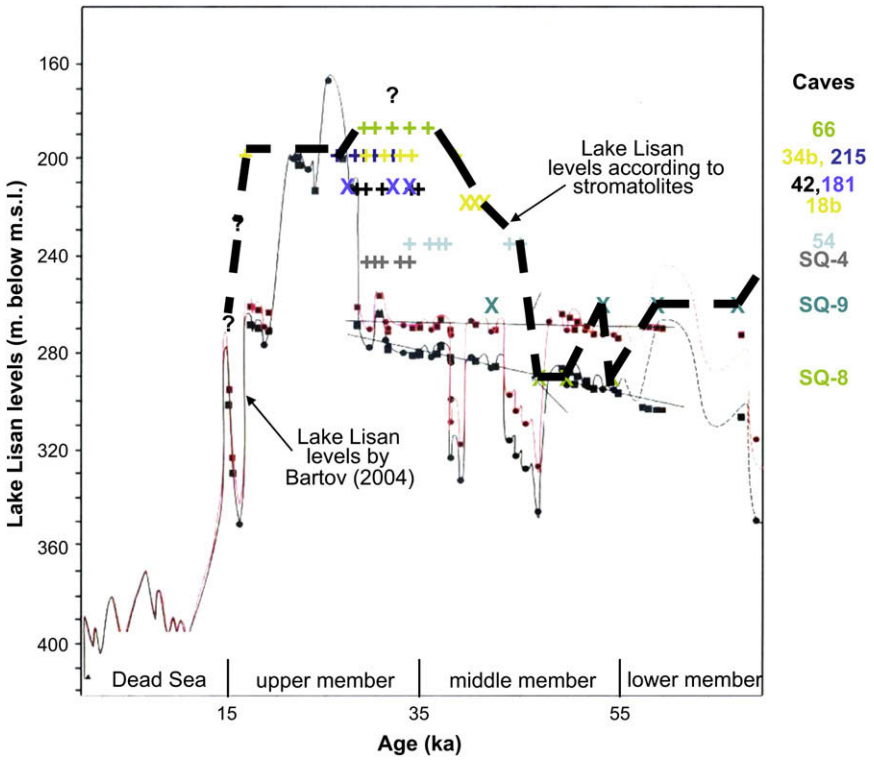


Fig. 10. Lake Lisan levels according to stromatolites from caves of the Fault Escarpment, compared to reconstruction of Lake Lisan levels by Bartov (2004).

for part of this time interval (Fig. 10), supporting the argument for relative stability of the escarpment compared to the downfaulted blocks within the Dead Sea basin.

The stromatolite levels correlative with Lake Samra to Lake Lisan transition, −247 and −262 m relative to m.s.l., at ~75–67.5 ka (Caves 72a and SQ-9), are up to 150 m higher compared to the lake levels reconstructed for this transition by Waldman (2002), i.e. ~−400 m. This difference suggests tectonic subsidence of intermediate blocks, up to 150 m/75 ka, i.e. up to 2 m/ka—a similar rate to that calculated for the last 35.6 ka.

Subsidence in the order of 2 m/ka is close to the average subsidence rates estimated by Begin and Zilberman (1997) for the Dead Sea basin: (a) 1.45 m/ka for the last 6 Ma (based on data by Zak and Freund, 1981); (b) 3.0 m/ka for the last 6 Ma (based on data by ten Brink and Ben-Avraham, 1989); (c) 2.3–5.45 m/ka for the last 2.0–1.8 Ma (based on data by Horowitz, 1989).

Tectonic activity in the Dead Sea depression indeed continued into the Pleistocene (Avni, 1998) and the Holocene (Reches and Hoexter, 1981), up to recent times (Eyal and Reches, 1983). This activity affected the Darga Conglomerate of Plio-Pleistocene age (Raz, 1983), the Samra Formation of Pleistocene age (Waldmann, 2002), the Lisan Formation of Upper Pleistocene age (Agnon, 1982; Raz, 1983; Avni, 1998), as well as Holocene sediments within the depression (Reches and Hoexter, 1981). Tectonic faults which were active during the last tens of thousands of years in the Dead Sea area are documented by Garfunkel et al. (1981). Faults younger than 15 ka were found to downfault rocks of the Lisan Formation by more than 25 m, i.e. 1.7 m/ka (Begin and Zilberman, 1997, based on data by Agnon, 1982)—close to the subsidence rates calculated above. Moreover, according to Ben-Avraham and Lazar (2006), faults reaching a total throw of a few kilometers, are buried under the depression's sedimentary fill, downfaulting Pleistocene units (Raz, 1983; Avni, 1998; Waldman, 2002).

Lake levels based on stromatolites dated 59–42 ka at the lowermost caves, i.e. SQ-9 and SQ-8 at −262 and −292 m relative to m.s.l., respectively, are similar to Lake Lisan levels reconstructed by Bartov (2004) for this time interval (Fig. 10). Both caves are located within a subsided structural block in the northern part of the Fault Escarpment, i.e. the Qumran area (Fig. 2B). It is thus reasonable to assume that the tectonic movement of this block, downfaulted the caves with stromatolites to levels similar to those of the Lisan Formation in the depression fill. Therefore, the lower altitudes of the stromatolites from Caves SQ-8 and SQ-9, and thus that part of the lake level curve between 59 and 42 ka (see Figs. 9 and 10), most probably do not represent the higher "original" lake level.

7. Summary and conclusions

A diverse array of stromatolites was encountered within caves along the Dead Sea Fault Escarpment. Their general resemblance to previously documented stromatolite occurrences in the area, as well as the altitudes (−310 to −188 m, relative to m.s.l.), ages (~75 to 17 ka), and aragonite mineralogy, ascribe them to Lake Lisan of Late Pleistocene age.

The stromatolites are considered to represent the lake levels, thus being markers of the water balance at the catchment area, and tectonic movements at the vicinity.

The stromatolite assemblage within the caves includes wavy-laminar deposits, often as "dome-shaped" (hemispheroidal) and "club-shaped" (columnar) structures, forming clusters of tens of laterally-linked closely-spaced individuals. Other morphologies include crusts, porous formations of irregular shape, and "coralloids". More than one of the above mentioned types were usually encountered within a single cave, occasionally as composite stromatolite structures.

The cave stromatolites display most of the characteristic microtextures and microstructures: aragonite crystals with radial-fibrous pattern and/or wavy extinction, micritic matter, laminoid fenestrae porosity, pelloids, and wavy lamination.

The preservation of the original structure and aragonite mineralogy of the stromatolites is indicative of a closed-system enabling accurate U–Th dating. A lake level curve was drawn based on the radiometric ages of the stromatolites (Fig. 9), representing the time span of the Lisan Formation. According to this curve, lake levels of ca. −250 m relative to m.s.l. were achieved at ~75–72.5 ka, and high stands above −220 m relative to m.s.l. were already achieved at 41.5 ka. These results indicate lake levels tens of meters higher than previously reconstructed (Fig. 10).

The discrepancies between the current lake level curve, whose data was gathered on the Fault Escarpment (Fig. 2B), and previous curves whose data was collected from the Lisan Formation in the depression fill east of the escarpment, are explained by subsidence of intermediate tectonic blocks within the depression relative to its margins. The calculated subsidence rate is up to 2–2.2 m/ka for the last 75 ka—on the same order of magnitude as previously calculated subsidence rates.

Stromatolite ages occurring tens of meters under the lake level curve can be representative of post-Lisan local subsidence of tectonic blocks within the escarpment, algae growing under the water surface, and/or lake level oscillations on a centennial to millennial scale. This curve is thus regarded as a minimum-stand pointer of the lake at any given time.

Acknowledgments

We would like to acknowledge the Dead Sea Research and Development Authority, the Israel Ministry of Science, Prof. Amos Nur of Stanford University (USA), and Israel Science Foundation grant no. 910/05, for the support of this study. We also thank the Cave Research Unit of the Geography Department of the Hebrew University of Jerusalem who participated in the cave survey, Mr. Eli Raz of the Dead Sea Research and Development Authority who contributed useful advice, and Dr. I. Segal and Mrs. N. Tepliakov of the Geological Survey of Israel who helped with the U–Th dating. Many thanks to the reviewers, Dr. A. Mangini, Dr. E. Zilberman, and an anonymous reviewer, and to the Editor, for their critical comments which helped improve the manuscript.

References

Agnon, A., 1981. Neogene Development of the Western Margin of the Southern Dead Sea Depression. Geological Survey of Israel Current Researches, 27–29.

Agnon, A., 1982. Post-Lisan faults in the Dead Sea Fault Escarpment. Israel Geological Society Annual Meeting, abstracts, p. 31.

Avni, Y., 1998. Paleogeography and Tectonics of the Central Negev and the Dead Sea Rift Western Margin During the Late Neogene and Quaternary. Geological Survey of Israel, Jerusalem, 231 pp.

Bar-Matthews, M., Ayalon, A., Kaufman, A., 1997. Late Quaternary paleoclimate in the eastern Mediterranean region from stable isotope analysis of speleothems in Soreq Cave, Israel. Quaternary Research 47, 155–168.

Bar-Matthews, M., Ayalon, A., Kaufman, A., Wasserburg, G.J., 1999. The Eastern Mediterranan paleoclimate as a reflection of regional events: Soreq Cave, Israel. Earth and Planetary Science Letters 166, 85–95.

Bartov, Y., 1999. The Geology of the Lisan Formation in the Masada plain and the Lisan Peninsula. M.Sc. thesis, Hebrew University of Jerusalem (in Hebrew with English abstract).

Bartov, Y., 2004. Sedimentary Fill Analysis of a Continental Basin—The Late Pleistocene Dead Sea. Ph.D. Thesis, The Hebrew University, Jerusalem, 114 pp (in Hebrew with English abstract).

Bartov, Y., Stein, M., Enzel, Y., Agnon, A., Reches, Z., 2002. Lake levels and sequence stratigraphy of Lake Lisan, the Late Pleistocene precursor of the Dead Sea. Quaternary Research 57, 9–21.

Bartov, Y.S., Goldstein, L., Stein, M., Enzel, Y., 2003. Catastrophic arid episodes in the Eastern Mediterranean linked with the North Atlantic Heinrich events. Geology 31 (5), 439–442.

Bartov, Y., Bookman, R., Enzel, Y., 2006. Current depositional environments at the Dead Sea margins as indicators of the past lake levels. In: Enzel, Y., Agnon, A.,

Stein, M. (Eds.), New Frontiers in Dead Sea Paleoenvironmental Research. Geological Society of America Special Publications, vol. 401, pp. 127–140.
Begin, Z.B., 1975. The geology of the Jericho sheet (geological map series 1:50,000). Geological Survey of Israel Bulletin 67.
Begin, Z.B., Zilberman, E., 1997. Main stages and Rate of the Relief Development in Israel, Geological Survey of Israel report, Jerusalem, 63 pp. (in Hebrew with English abstract).
Begin, Z.B., Ehrlich, A., Nathan, Y., 1974. The Lisan Lake, the Pleistocene precursor of the Dead Sea. Geological Survey of Israel Bulletin 63.
Begin, Z.B., Nathan, Y., Ehrlich, A., 1980. Stratigraphy and facies distribution in the Lisan Formation—new evidence from the area south of the Dead Sea, Israel. Israel Journal of Earth Sciences 29, 182–189.
Begin, Z.B., Broecker, W., Buchbinder, B., Druckman, Y., Kaufman, A., Magaritz, M., Negev, D., 1985. Dead Sea and Lake Lisan levels in the Last 30,000 Years: A Preliminary Report. Geological Survey of Israel report, Jerusalem, 18 pp.
Ben-Avraham, Z., Lazar, M., 2006. The structure and development of the Dead Sea basin: Recent studies. In: Enzel, Y., Agnon, A., Stein, M. (Eds.), New Frontiers in Dead Sea Paleoenvironmental Research. Geological Society of America. Special Papers, vol. 401, pp. 1–13.
Ben-Avraham, Z., Niemi, T.M., Neev, D., Hall, J.K., Levy, Y., 1993. Distribution of Holocene sediments and neotectonics in the deep north basin of the Dead Sea. Marine Geology 113, 219–231.
Bender, F., 1974. Geology of Jordan, Contributions to the Regional Geology of the Earth. Gebruder Borntraeger Berlin, Stuttgart.
Bentor, Y.K., Vroman, A., 1957. Geological Map of Israel, 1:100,000, sheet 19—Ha'Arava. Geological Survey of Israel, Jerusalem.
Bentor, Y.K., Vroman, A., 1960. Geological Map of Israel, 1:100,000, Series A, Sheet 16—The Negev: Mount Sdom, Explanatory Text. Geological Survey of Israel, Jerusalem, 117 pp.
Bookman (Ken-tor), R., Enzel, Y., Stein, M., Agnon, A., 2004. Late Holocene lake levels of the Dead Sea. Geological Society of America Bulletin 116 (5), 555–571.
Bowman, D., 1997. Geomorphology of the Dead Sea western margin. In: Niemi, T.M., Ben-Avraham, Z., Gat, Y. (Eds.), The Dead Sea—The Lake and its Setting. Oxford University Press, pp. 217–225.
Bowman, D., Gross, T., 1992. The highest stand of Lake Lisan: ~150 meter below MSL. Israel Journal of Earth Sciences 41, 233–237.
Buchalo, A.S., Nevo, E., Wasser, S., Oren, A., Molitoris, H.P., 1998. Fungal life in the extremely hypersaline water of the Dead Sea: first records. Proceedings of the Royal Society of London 265, 1461–1465.
Buchbinder, B., 1981. Morphology, microfabric, and origin of stromatolites of the Pleistocene precursor of the Dead Sea, Israel. In: Monty, C. (Ed.), Phanerozoic Stromatolites; Case Histories. Springer-Verlag, Berlin, pp. 181–196.
Buchbinder, B., Begin, B.Z., Friedman, G.M., 1974. Pleistocene algal tufa of Lake Lisan, Dead Sea area. Israel. Israel Journal of Earth Sciences 23, 131–138.
Druckman, Y., 1981. Sub-recent Manganese-bearing stromatolites along shorelines of the Dead Sea. In: Monty, C. (Ed.), Phanerozoic Stromatolites; Case Histories. Springer-Verlag, Berlin, pp. 197–208.
Elron, A., 1980. The Geology of the Lower Na'chal Zin. M.Sc. Thesis. The Hebrew University, Jerusalem (in Hebrew, with English abstract).
Enzel, Y., Amit, R., Dayan, U., Crouvi, O., Kahana, R., Ziv, B., Sharon, D., 2008. The climatic and physiographic controls of the eastern Mediterranean over the late Pleistocene climates in the southern Levant and its neighboring deserts. Global and Planetary Changes 60, 165–192.
Eyal, Y., Reches, Z., 1983. Tectonic analysis of the Dead Sea Rift region since the Late Cretaceous based on mesostructures. Tectonics 2, 167–185.
Frumkin, A., 1997. The Holocene history of the Dead Sea levels. In: Niemi, T.M., Ben-Avraham, Z., Gat, Y. (Eds.), The Dead Sea—The Lake and its Settings. Oxford University Press, pp. 237–248.
Frumkin, A., 2000. Karst and caves of Israel. In: Decu, V., Juberthie, C. (Eds.), Encyclopedia Biospeologica 3. Société de Biospéologie, Bucharest, pp. 1840–1842.
Frumkin, A., 2001. The Cave of the Letters sediments—indication of an early phase of the Dead Sea depression? Journal of Geology 109, 79–90.
Frumkin, A., Kadan, G., Enzel, Y., Eyal, Y., 2001. Radiocarbon chronology of the Holocene Dead Sea: attempting a regional correlation. Radiocarbon 43 (3), 1179–1189.
Garfunkel, Z., 1978. The Negev: regional synthesis of sedimentary basins, 10th International Congress of Sedimentology, part I, Precongress, Israel, pp. 35–110.
Garfunkel, Z., 1981. Internal structure of the Dead Sea leaky transform (rift) in relation to plate kinematics. Tectonophysics 80, 81–108.
Garfunkel, Z., 1997. The history and formation of the Dead Sea basin. In: Niemi, T.M., Ben-Avraham, Z., Gat, Y. (Eds.), The Dead Sea—The Lake and its Setting. Oxford University Press, pp. 36–56.
Garfunkel, Z., Horowitz, A., 1966. The Upper Tertiary and Quaternary morphology of the Negev. Israel Journal of Earth Sciences 15, 101–117.
Garfunkel, Z., Zak, I., Freund, R., 1981. Active faulting in the Dead Sea rift. Tectonophysics 80, 1–26.
Haase-Schramm, A., Golstein, S.L., Stein, M., 2004. U–Th dating of Lake Lisan (Late Pleistocene Dead Sea) aragonite and implications for glacial East Mediterranean climate change. Geochimica et Cosmochimica Acta 68 (5), 985–1005.
Horowitz, A., 1987. Palynological evidence for the age and rate of sedimentation along the Dead Sea Rift, and structural implications. Tectonophysics 141, 107–116.
Horowitz, A., 1989. Palynological evidence for the Quaternary rates of accumulation along the Dead Sea Rift, and structural implications. Tectonophysics 164, 63–71.
Kadan, G., 1997. Evidence for Dead Sea Lake-Level Fluctuations and Recent Tectonism from the Holocene Fan-Delta of Nahal Darga, Israel. M.Sc.Thesis, Ben-Gurion University of the Negev, Beer-Sheva, Israel (in Hebrew, with English abstract).
Kaufman, A., Yechieli, Y., Gardosh, M., 1992. Reevaluation of the lake-sediment chronology in the Dead Sea basin, Israel, based on new ^{230}Th/U dates. Quaternary Research 38, 292–304.
Kaufman, A., Wasserburg, G.J., Porcelli, D., Bar-Matthews, M., Ayalon, A., Halicz, L., 1998. U–Th isotope systematics from the Soreq cave, Israel, and climatic correlations. Earth and Planetary Science Letters 156, 141–156.
Kolodny, Y., Stein, M., Machlus, M., 2005. Sea-rain-lake relation in the Last Glacial East Mediterranean revealed by δ^{18}O-δ^{13}C in Lake Lisan aragonites. Geochimica et Cosmochimica Acta 69 (16), 4045–4060.
Langozky, Y., 1963. High-level lacustrine sediments in the Rift Valley at Sdom. Israel Journal of Earth Sciences 12, 17–25.
Logan, B.W., Rezak, R., Ginsburg, R.W., 1964. Classification and environmental significance of algal stromatolites. Journal of Geology 72, 68–81.
Machlus, M., Enzel, Y., Goldstein, S.L., Marco, S., Stein, M., 2000. Reconstructing low-levels of Lake Lisan by correlating fan-delta and lacustrine deposits. Quaternary International 73/74, 127–144.
Manspeizer, W., 1978. The Dead Sea marginal sedimentary facies. In: Schulman, N., Bartov, Y. (Eds), Tectonics and Sedimentation along the Rift Valley, 10th International Congress of Sedimentology, part II: Postcongress, Israel, pp. 51–55, 76-79.
Manspeizer, W., 1985. The Dead Sea Rift: impact on climate and tectonism on Pleistocene and Holocene sedimentation. In: Biddle, K.T., Christie-Black, N. (Eds.), Strike-Slip Deformation, Basin Formation and Sedimentation. Society of Economic Paleontology and Mineralogy, Special Publication, 37, pp. 143–158.
Martinson, D.G., Pisias, N.G., Hays, J.D., Imbrie, J., Moore, T.C., Shackleton, N.J., 1987. Age dating and the orbital theory of the ice ages: Development of a high-resolution 0 to 300,000-year chronostratigraphy. Quaternary Research 27, 1–29.
Migowski, C., Stein, M., Prasad, S.J., Negendank, F.W., Agnon, A., 2006. Holocene climate variability and cultural evolution in the Near East from the Dead Sea sedimentary record. Quaternary Research 66 (3), 421–431.
Monty, C., 1981. Spongiostromate vs. porostromate stromatolites and oncolites. In: Monty, C. (Ed.), Phanerozoic Stromatolites; Case Histories. Springer-Verlag, Berlin, pp. 1–4.
Mor, O., 1987. The Geology of the Judean Desert in the Na'chal Darga Area. MSc. Thesis, The Hebrew University, Jerusalem, 112 pp. (in Hebrew, with English abstract).
Mor, O., Burg, A., 2000. Geological Map of Israel, Sheet 12-III, Mizpe Shalem, 1:50,000. Geological Survey of Israel, Jerusalem.
Neev, D., Emery, K.O., 1967. The Dead Sea, depositional processes and environment of evaporates. Geological Survey of Israel Bulletin 41.
Neev, D., Hall, J.K., 1977. Climatic fluctuations during the Holocene as reflected by the Dead Sea levels, Presented at the international conference on terminal lakes, Ogden, Oregon, USA. Geological Survey of Israel, Jerusalem, 8 pp.
Neev, D., Langozky, Y., 1961. Tufa deposits (algal bioherms?) of the Lisan Lake. In: Symposium on the Pleistocene in Israel. Association for the Advancement of Science in Israel, The Hebrew University, Jerusalem, pp. 10-11(in Hebrew).
Niemi, T.M., 1997. Fluctuations of Late Pleistocene Lake Lisan in the Dead Sea Rift. In: Niemi, T.M., Ben-Avraham, Z., Gat, Y. (Eds.), The Dead Sea—The Lake and its Setting. Oxford University Press, pp. 226–248.
Niemi, T.M., Ben-Avraham, Z., 1997. Active tectonics in the Dead Sea basin. In: Niemi, T.M., Ben-Avraham, Z., Gat, Y. (Eds.), The Dead Sea—The Lake and its Setting. Oxford University Press, pp. 73–81.
Pia, J., 1933. Die Rezentem Kalksteinen. Akademische Verlagsgesellschaft M.B.H., Berlin, 420 pp.
Picard, L., 1931. Geological Researches in the Judean Desert. Ph.D Thesis, The Hebrew University, Jerusalem.
Picard, L., 1943. Structure and Evolution of Palestine. Geological Department, The Hebrew University, Jerusalem, 134 pp.
Plakht, J., Sheinkman, V., Shlukov, A., 2002. Age of the Lisan sediments: new TL-data and interpretation. Israel Geological Society Annual Meeting Abstracts, Ma'agan, 2002, p. 91.
Raab, M., Friedman, G.M., Spiro, B., Starinsky, A., Zak, I., 1997. The geological history of Messinian (Upper Miocene) evaporites in the Central Jordan Valley (Israel) and how strontium and sulfur isotopes relate to their origin. Carbonates and Evaporites 12, 296–324.
Raz, E., 1983. The Geology of the Judean Desert, En-Gedi Area. Geological Survey of Israel, Jerusalem, 110 pp (in Hebrew, with English abstract).
Raz, E., 1986. Geological Map of Israel, Sheet 16-I, En-Gedi, 1:50,000. Geological Survey of Israel, Jerusalem.
Reches, Z., Hoexter, D.F., 1981. Holocene seismic and tectonic activity in the Dead Sea area. Tectonophysics 80, 235–254.
Roth, I., 1970a. The Geology of Wadi el-Qelt Area. M.Sc. Thesis, The Hebrew University, Jerusalem (in Hebrew).
Roth, I., 1970b. Geological Map of Wadi el-Qelt. Sheet 12-I. Geological Survey of Israel, Jerusalem.
Sagy, A., Reches, Z., Agnon, A., 2003. Hierarchic three-dimensional structure and slip partitioning in the western Dead Sea pull-apart. Tectonics 22 (1), 1004.
Schramm, A., Stein, M., Goldstein, S.L., 2000. Calibration of the ^{14}C time-scale to >40 ka by ^{234}U-^{230}Th dating of Lake Lisan sediments (last glacial Dead Sea). Earth and Planetary Science Letters 175, 27–40.
Schwarcz, H.P., 1986. Geochronology and isotopic geochemistry of speleothems. In: Fritz, Fontes (Ed.), Handbook of Environmental Isotope Geochemistry. The Terrestrial Environment, Vol. 2. Elsevier, Amsterdam. pp. 271–303.
Shahar, Y., Reiss, Z., Gerry, E., 1966. A new outcrop of marine Neogene in the Negev. Israel Journal of Earth Sciences 15, 82–84.

Shaliv, G., 1991. Stages in the tectonic and volcanic history of the Neogene basin in the Lower Galilee and the valleys. Geological Survey of Israel, Jerusalem, 94 pp.
Shamir, G., 2006. The active structure of the Dead Sea Depression. In: Enzel, Y., Agnon, A., Stein, M. (Eds.), New Frontiers in Dead Sea Paleoenvironmental Research. Geological Society of America Special Papers, vol. 401, pp. 15–32.
Sneh, A., 1979. Late Pleistocene Fan-Deltas along the Dead Sea Rift. Journal of Sedimentary Petrology 49, 541–552.
Stein, M., 2001. The sedimentary and geochemical record of Neogene—Quaternary water bodies in the Dead Sea Basin—inferences for the regional paleoclimatic history. Journal of Paleolimnology 26, 271–282.
Stein, M., Starinsky, A., Katz, A., Goldstein, S.L., Machlus, M., Schramm, A., 1997. Strontium isotopic, chemical, and sedimentological evidence for the evolution of Lake Lisan and the Dead Sea. Geochimica et Cosmochimica Acta 61 (18), 3975–3992.
Steinitz, G., Bartov, Y., 1991. The Miocene–Pliocene history of the Dead Sea segment of the rift in light of K-Ar ages of basalts. Israel Journal of Earth Sciences 40, 199–208.
ten Brink, U.S., Ben-Avraham, Z., 1989. The anatomy of a pull-apart basin: seismic reflection observations of the Dead Sea basin. Tectonics 8, 333–350.
Vaks, A., Bar-Matthews, M., Ayalon, A., Matthews, A., Frumkin, A., Dayan, U., Halicz, L., Almogi-Labin, A., Schilman, B., 2006. Paleoclimate and location of the border between Mediterranean climate region and the Saharo-Arabian Desert as revealed by speleothems from the northern Negev Desert, Israel. Earth and Planetary Science Letters 249, 384–399.
Waldmann, N., 2002. The Geology of the Samra Formation of the Dead Sea Basin. MSc. Thesis, The Hebrew University, Jerusalem (in Hebrew, with English abstract).
Waldmann, N., Starinsky, A., Stein, M., 2007. Primary carbonates and Ca-chloride brines as monitors of a paleo-hydrological regime in the Dead Sea basin. Quaternary Science Reviews 26 (17-18), 2219–2228.
Weinberger, R., Bar-Matthews, M., Levi, T., Begin, Z.B., 2007. Late Pleistocene rise of the Sedom diapiron the backdrop of water-level fluctuations of Lake Lisan, Dead Sea basin. Quaternary International 175 (1), 53–61.
Zak, I., 1967. The Geology of the Sedom Mountain. Ph.D. Thesis. The Hebrew University. Jerusalem (in Hebrew).
Zak, I., Freund, R., 1981. Asymmetry and basin migration in the Dead Sea rift. Tectonophysics 80, 27–38.